Turkish Journal of Science & Technology
Volume 13(2), 1-13, 2018

The Effects of The Perforation Shapes, Sizes, Numbers and Inclination Angles on The Thermal Performance of A Perforated Pin Fin

Hisham H. Jasim[1,2] and Mehmet Sait Söylemez[1]
[1] Department of Mechanical Engineering**,** University of Gaziantep, 27310 Gaziantep, Turkey
[2] University of Baghdad, Baghdad, Iraq
ha19211@mail2.gantep.edu.tr, enghisham78@yahoo.com

(Geliş/Received: 03.04.2017; Kabul/Accepted: 22.04.2018)

Abstract

Many of the proposed methods introduced the perforated fin with the straight direction to improve the thermal performance of the heat sink. Present rectangular pin fin consists, innovative form of the perforation (with inclination angles). To investigate the thermal behavior of the present model, changes in each of the geometric consideration (shape, size and number of perforations) and inclination angles were considered. Signum function is used for the modeling the opposite and the mutable approach of the heat transfer area. The Degenerate Hypergeometric Equation (DHE) was used as a new derivative method to find the general solution, then solved by Kummer's series. Two validation ways (previous work and Ansys 16.0-Steady State Thermal) are considered. The present mathematical model has big reliability according to the high agreement of the validation results about (0.31%- 0.60%). Also, the results show a decrease of the fin temperature as a result of the increase the heat transfer area. It was found, use of the perforated fin leads to decrease the thermal resistance and improve the thermal performance of the pin fin by enhancing the heat transfer and increase the effectiveness.

Keywords: Perforated fin, Incline perforation, Natural convection, Heat transfer enhancement, Performance analysis.

Perforeli Kanatlarda Şekil, Boyut Ve Eğim Açısının Isıl Performansa Etkisi

Özet

Bu çalışma elektronik parçaların soğutulmasında kullanılan perforeli kanatların ısıl performansını arttırmak için yapılmıştır. Dörtgen kesitli kanatlar için değişik tarzda eğimli bir perforeli kanat konusunda yeni ve orijinal sonuçlar elde edilmiştir. Mevcut modelin ısıl performans üzerindeki etkileri detaylı olarak araştırılmış ve sunulmuştur. Çalışmada teorik çözüm için Signum Fonksiyonu kullanılmıştır. Dejeneratf Hipergeometrik Denklemi ile birlikte Kummer's Serisi kullanılarak genel çözüm elde edilmiştir. Mevcut sonuçlar ANSYS 16.0 ve sürekli rejim sonuçları ile mukayese edilerek doğrulanmıştır. Sonuçlar arasında bide üç ile altı mertebesinde farklılık görülmüştür. Ayrıca, sonuçlar ısı transfer alanının artmasıyla kanat sıcaklığının azaldığını göstermektedir. Perforasyon etkisi ile ısıl direncin azaldığı ve bu nedenle ısıl performansın yani kanat etkenlik değerinin arttığı gözlenmiştir.

Anahtar Kelimeler: Perforeli kanat, Eğimli perforasyon, Doğal taşınım, Isı transfer artışı, Isıl performans.

1. Introduction

Modern development leads to closely positioned components and high densities of electrical power [1]. That's meaning, should be increase the heat transfer from the heat sink. For this reason, the investigators used the perforation towards straight direction to improve the thermal resistance. Moreover, the changes of the shapes, sizes, numbers and orientation of the perforations were adopted to optimize the thermal performance.

Computational technique is used by the most investigators to solve the governing equations. Five cases with single perforation and three cases with multiple perforations of an annular finned-tube system were evaluated to find the best performance by [2] in extreme climatic conditions, a single perforation location at 120^o provided the favorable results. Also, the enhancement of the heat transfer can be reached to the 5.96%.

Circular, rectangular and trapezoidal cross section area of the perforation was studied by [3]

to find the effects of the number and geometry of the hollow fin on the heat transfer through rectangular fins attached to microchannel heat sink, results show the improvement is strongly depends on the numbers of the hollows and negligible influence of the hollow geometry. To show the advantages of the perforation, [4] shows The thermal profile of the perforated fins in a staggered manner performs better than the solid elliptical pin fin according to the Static temperature, Nusselt number and total heat that is calculated.

The effects of the porosity on the performance of the fins were investigated by [5,6] for longitudinal and lateral perforation. Rectangular cross section with different dimensions and multi numbers of the perforation was considered to show the thermal enhancement at various operating conditions. Higher performances for perforated fins are observed. Also the increased effectiveness by increasing porosity ratio.

The Nusselt Number and the friction factor were optimized separately and together for the circular perforated of the rectangular cross section by [7], the results show the higher thermal performance of the pin fin dependent on the lower clearance ratio and lower inter-fin spacing ratio also the efficiency can be increased by 1.1 and 1.9 based on the Reynolds numbers. Likewise, the pin fin efficiency of the circular cross section can be increased by 1.4 and 1.6 by using the circular perforation and the Nusselt number having inversely proportional to the clearance ratio and inter-fin spacing ratio according to [8,9]. A copper material possesses higher thermal conductivity when compared with other material by [10], also a large number of perforated were given the higher heat transfer coefficient.

The larger hollow pin diameter ratio, offered higher augmentation factor for upward orientation, and the situation was reversed for sideward orientation for the circular pin fin using the circular perforation that are studied by [11].

The Reynolds number and size of perforation have a larger impact on the Nusselt number for rectangular fin using the lateral perforations (square and circular) that are presented by [12]. Perforated pin fin in the cylindrical channel was tested by change the number of a circular perforation, The results show the number of perforations has the significant increase of the convective heat transfer about (30% to 40%) [13].

Other investigations found the temperature distribution of perforated fin by analytical study,[14] reached to the temperature distribution equation of perforated flat plate based on the mathematical model that solved by Fourier series and Flocke's theory. [15] reported the decrease of thermal conduction resistance of pin fin due to triangular perforation, which leads to improved the heat dissipation that calculated by use variation approach, finite element techniques.

Likewise, [16] applied the same technique to find the effects of the orientations of the rectangular perforations under natural convection, the results show the inclined orientation is better for low each of the thickness and thermal conductivity while the parallel orientation is better for higher thickness. Also, [17] concluded to enlarge of perforated size and increase the thermal conductivity leads to augmentation the heat transfer from the rectangular fin.

In [18] the optimization of the thermal resistance was performed on pin-fin heat sinks with a constant Reynolds number. The results show increased the number of the fin leads to decrease the thermal resistance without limit for height (40 mm) while the optimum number of fins can be found at the height (20mm and 30mm).

New approach introduced in this article, by proposing two novelty points, firstly at geometric model, the incline perforation is considered. Secondly, at Analytical process, the new differential technique is used to derive the general form of the temperature distribution regardless of the perforation shape. Also, the Signum function is used for modeling the opposite and the mutable approach of the heat transfer area. After that, the effects of the incline perforated on the thermal performance can be studied.

2. Geometric Model

The incline perforated region of the pin fin is shown in Figure 1. In the general form, an

undefined section of perforation was considered. Inclination started from ($\beta = 0$) at straight perforation. The fin has a rectangular cross section area with one and two perforations. Also, the base fin is located at the x-z plane and y-axis at the fin length. Due to the incline perforation, the heat transfer area is changing with y-direction as well as change with the inclination angle.

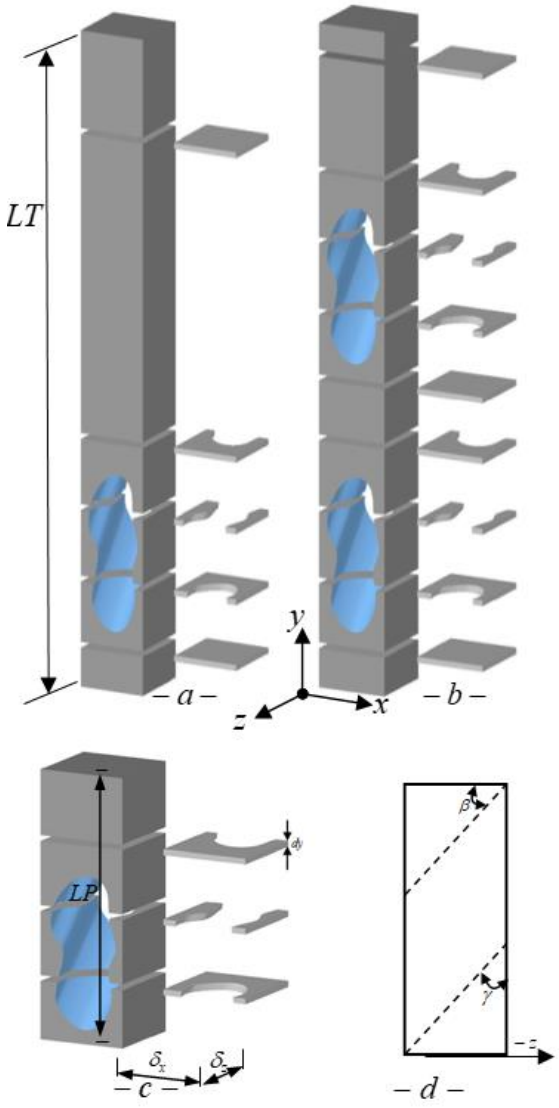

Figure 1. Fin with incline perforated. a- fin one perforation. b- fin with two perforations. c- 3-D model of the perforated region with different layer. d- side view.

3. Energy Analysis and Assumption

Energy balance is applied to the element shown in Figure 2, to obtain the differential equation of energy (1) in the perforated region.

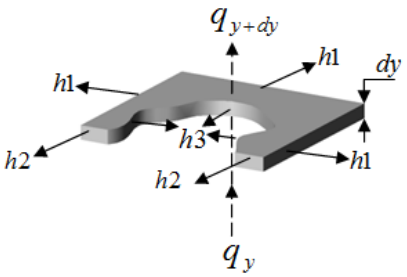

Figure 2. Element description

In this study, heat transfer analysis relies on a set of assumptions:

1- Steady heat conduction with no heat generation.
2- One-dimensional heat transfer analysis depended on the impairment of the Biot number at z-axis and x-axis.
3- Constant conductivity ($k = 222$ $W/m.K$,(A1050)).
4- Constant base temperature.
5- Insulation tip fin, radiation effects are neglected.
6- Uniform ambient temperature and uniform convection heat transfer coefficient.
7- Convection coefficient is divided into three types (external non-perforated (h1), external perforated (h2) and internal perforated (h3)).

$$\frac{d}{dy}(A_{cond.}\frac{d\theta}{dy})dy = [h1P_{conv1} + h2P_{conv2} + h3P_{conv3}]\frac{\theta\, dy}{k} \quad (1)$$

$$\theta = T(y) - T_{air}$$

Where A_{cond} is the conduction area, P_{conv} is the perimeter of the convection. Various convection heat transfer coefficients were appeared due to incline perforation. Moreover, Convection coefficients depended on the properties of cooling fluid, specifications of the perforated fin and the open perforated ratio (ROP). ROP represents the ratio of actual perforated area to maximum perforation effects. Convection coefficients h1, h2 and h3 were calculated according to the ref. [19 , 20,21], respectively.

4. General Solution

Equation (1) can be represented by use the Degenerate Hypergeometric Equation (DHE)[22,23].

$$\vartheta \frac{d^2u}{d\vartheta^2} + (ku1 - \vartheta)\frac{du}{d\vartheta} - (ku2)\,u = 0 \qquad (2)$$

Where: $u = e^{\vartheta/2}G$, $\vartheta = \xi^2\sqrt{p1}$,

$$\theta = G/\sqrt{A_{cond.}} \ , \xi = y + \frac{p2}{2p1}$$

$ku1, ku2$ = constants .

The DHE equation (2) was solved by Kummer's series [24,25] to get the general solution of the present model.

$$u(\vartheta) = CO_i\ \phi(ku1, ku2, \vartheta) + CO_{i+1}\ \psi(ku1, ku2, \vartheta) \quad , i = 1,3,5,.... \qquad (3)$$

Where:

ϕ = confluent hypergeometric function of the first kind.

ψ = confluent hypergeometric function of the second kind.

CO = Constant for the general solution.

Boundary conditions, for the constant base temperature:

$$u\big|_{\vartheta=\frac{p2^2}{4\,p1^{3/2}}} = \theta_b\sqrt{A_b}\,e^{\frac{p2^2}{8\,p1^{3/2}}} \quad , \left.\frac{du}{d\vartheta}\right|_{\vartheta=(LP+\frac{p2}{2p1})^2\sqrt{p1}} = 0$$

Which compatible to the boundary conditions at original form.

$$\theta\big|_{y=0} = \theta_b \quad , \left.\frac{d\theta}{dy}\right|_{y=LP} = 0$$

Solve of the equation (3) with above boundary conditions, which leads to the temperature distribution equation.

$$\frac{\theta(y)}{\theta_b} = \frac{e^{\frac{-(y+\frac{p2}{2p1})^2\sqrt{p1}}{2}}}{\sqrt{A_{cond.}}}\ [\zeta 10\ \phi(ku1, ku2, ((y+\frac{p2}{2p1})^2\sqrt{p1})) - \zeta 11\ \psi(ku1, ku2, ((y+\frac{p2}{2p1})^2\sqrt{p1}))] \qquad (4)$$

Where: $p1,2,...$ Constant [22]

$$\zeta 10 = \frac{\zeta 4\zeta 6 + \zeta 8\zeta 9}{\zeta 1\zeta 2(\zeta 4\zeta 6 + \zeta 8\zeta 9) - \zeta 1\zeta 3(\zeta 4\zeta 5 + \zeta 7\zeta 9)}$$

$$\zeta 11 = \frac{\zeta 4\zeta 5 + \zeta 7\zeta 9}{\zeta 4\zeta 6 + \zeta 8\zeta 9}\zeta 10$$

$$\zeta 1 = \frac{e^{\frac{-p2^2}{8\,p1^{3/2}}}}{\sqrt{A_b}} \quad , \quad \zeta 2 = \phi(ku1, ku2; \frac{p2^2}{8\,p1^{3/2}})$$

$$\zeta 3 = \psi(ku1, ku2; \frac{p2^2}{8\,p1^{3/2}}) \ , \ \zeta 4 = \frac{e^{\frac{-(LP+\frac{p2}{2p1})^2\sqrt{P1}}{2}}}{\sqrt{A_{cond.})_{LP}}}$$

$$\zeta 5 = \phi'[ku1, ku2; ((LP+\frac{p2}{2p1})^2\sqrt{p1})]$$

$$\zeta 6 = \psi'[ku1, ku2; ((LP+\frac{p2}{2p1})^2\sqrt{p1})]$$

$$\zeta 7 = \phi(ku1, ku2; ((LP+\frac{p2}{2p1})^2\sqrt{p1}))$$

$$\zeta 8 = \psi(ku1, ku2; ((LP+\frac{p2}{2p1})^2\sqrt{p1}))$$

$$\zeta 9 = -\frac{(LP+\frac{p2}{2p1})(\sqrt{p1}\sqrt{A_{cond})_{LP}})\ e^{\frac{-(LP+\frac{p2}{2p1})^2\sqrt{P1}}{2}}}{A_{cond})_{LP}} - \frac{\frac{A'_{cond.})_{LP}\ e^{\frac{-(LP+\frac{p2}{2p1})^2\sqrt{P1}}{2}}}{2\sqrt{A_{cond})_{LP}}}}{A_{cond})_{LP}}$$

5. Modeling of The Heat Transfer Area

In this study, two shapes of perforation (elliptical and rectangular) were considered. The change of the heat transfer area (Conduction area $A_{cond.}$ and convection perimeter $P_{conv.}$) is depending on the two parameters (y-axis and inclination angle), which leads to many difficulties when calculated the area at any specification. Likewise, the extreme ends for $A_{cond.}$ and $P_{conv.}$ can be represented by a point or

by a line depended on the inclination angle as shown in figure (3).

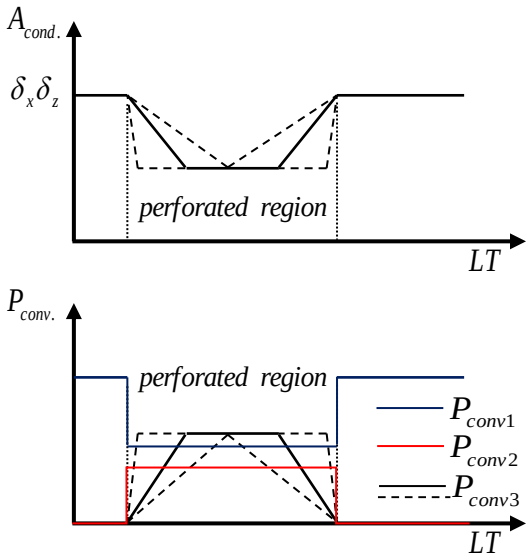

Figure 3. Change of the heat transfer area (conduction area and convection perimeter).

Signum function (sgn) [26] is used to represent the opposite and the mutable approach of variables $A_{cond.}$ and $P_{conv.}$. In case of the elliptical perforation ,figures (4 and 5) show the change of the perforated section with the y-axis based on the inclination angle. The equations of heat transfer area are derivative and formulated based on the group of the constants (a, a_1, a_2) as shown in the table (1). Moreover, equations (5– 8) are used to calculate the heat transfer area at any specification. In case of the rectangular perforation, ref.[22 and 23] was adopted.

$$A_{cond.} = \frac{AA}{a}(a_1 - y)\,\mathrm{sgn}(a - y) + (\delta_z\,\delta_x) - AA \qquad (5)$$

$$P_{conv1} = 2\,\delta_z + a_2 \qquad (6)$$

$$P_{conv2}\,dy = \int_{-b3}^{b3} (\delta_x - 2r\sqrt{1 - \frac{y^2}{b3^2}})\,dy \qquad (7)$$

$$P_{conv3} = 4\int_0^{w1} \sqrt{(r^2\cos^2\Omega) + (b2^2\sin^2\Omega)}\;d\Omega \qquad (8)$$

Where:

$$\mathrm{sgn}(a - y) = \tanh[(N(a - y)], \quad N >> 1$$

$$zp = z + \frac{\delta_z}{2}$$

$$w1 = \tan^{-1}\frac{\delta_z/2}{r\sqrt{1 - \frac{(\delta_z/2)^2}{b2^2}}}, \quad a = \delta_z \tan\beta$$

$$AA = (\pi\, r\, b2) - 4r\int_{-b2}^{-\delta_z/2} \sqrt{1 - \frac{zp^2}{b2^2}}\;dzp$$

$$b2 = \frac{1}{2}(\delta_z + \frac{2r - \delta_z \sin\beta}{\cos\beta}\tan\gamma), b3 = r/\cos\beta$$

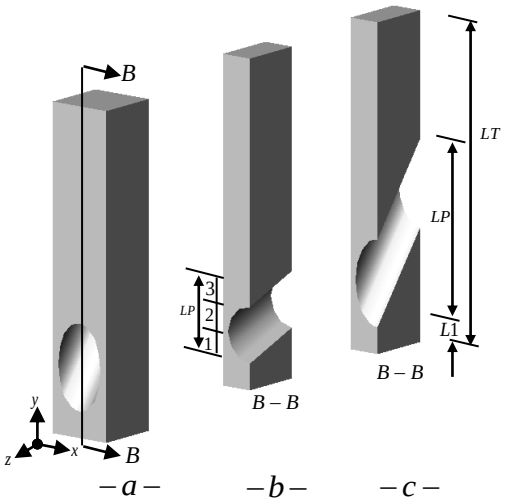

Figure 4. Ellipse perforated with different angle *a)* 3-D plot b) smaller angle c) bigger angle.

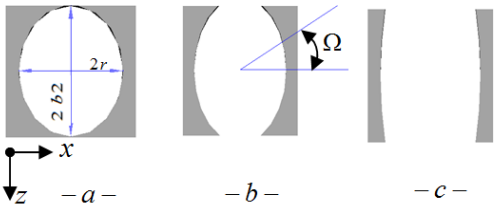

Figure 5. Ellipse section of perforated at a) bigger angle b) smaller than a c) smaller than b.

Table 1. Constant value

Region No.	Constant value	
	a_1	a_2
1	a	δ_x
2	y	0
3	LP-a	δ_x

In each shape of perforation, results of the two models (I and II) are calculated with natural convection, at a certain Rayleigh number ($Ra=10^6$). Models, I and II are described as follows:

Model I, elliptical perforation :

$\delta_x = \delta_z = 0.01\,(m),\ r = 0.0035(m),$

$LT = 0.05(m)$

Model II, elliptical perforation :

$\delta_x = \delta_z = 0.01\,(m),\ r = 0.004(m),$

$LT = 0.05(m)$

Model I, rectangular perforation:

$\delta_x = \delta_z = 0.01\,(m),\ bx = by = 0.007(m)$,

$LT = 0.05(m)$

Model II, rectangular perforation :

$\delta_x = \delta_z = 0.01\,(m),\ bx = by = 0.008(m),$

$LT = 0.05(m)$

6. Numerical Solutions and Simulation

The language of Matlab (R2014a) was used to calculate the thermal parameters based on the analytical solution. While, thermal analysis have been simulated by using -Ansys 16.0-Steady State Thermal- for all cases that are adopted in this study. Several grids are studied to ensure that the solutions are independent grids as shown in the tables (2 and 3) for the elliptical perforation and tables (4 and 5) for the rectangular perforation. The more accurate grid is required for the perforated region due to curvatures and edges. This problem is solved by changing the advanced size function to be proximity and curvatures, also the face size is calculated according to equation (9).

$$\text{Max. Face size} = \frac{\delta_x \text{ or } \delta_z}{NG}\ ,\ NG = 20-30 \quad (9)$$

The minimum temperature was compared until independent grids were succeeded. All the results are calculated at the base temperature (90 $^{\circ}C$) and air temperature (25 $^{\circ}C$). Two cases (case -1- and case -2-) were adopted to show the grid configurations as shown in figures (6 and 7) for the elliptical perforation and figures (8 and 9) for the rectangular perforation. The descriptions of two cases are shown below:

Case-1- model I with one perforation; Case-2- model II with two perforations.

Table 2. Grid independent studies

Inclination angle		Grid	Min. Temperature
Case-1-	β=8	115901	87.1
		137423	87.69
		148908	87.939
		158390	87.945
	β=22	129236	86.882
		147208	87.121
		160411	87.649
		172179	87.66

Table 3. Grid independent studies

Inclination angle		Grid	Min. Temperature
Case-2-	β=9	119932	85.86
		142111	86.24
		160854	86.528
		171546	86.53
	β=25	190234	85.29
		211906	85.78
		219523	86.16
		231248	86.18

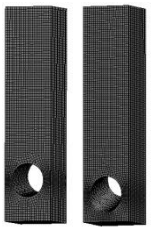

$-a-$ $-b-$

Figure 6. Grid configuration for the case -1- a) $\beta = 8$ b) $\beta = 22$

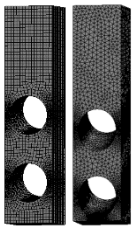

$-a-$ $-b-$

Figure 7. Grid configuration for the case -2- a) $\beta = 9$ b) $\beta = 25$.

Table 4. Grid independent studies

Inclination angle		Grid	Min. Temperature
Case-1-	β=8	131901	87.11
		150423	87.58
		162908	87.89
		172530	87.907
	β=22	140236	86.419
		158208	86.92
		171411	87.351
		183371	87.38

Table 5. Grid independent studies

Inclination angle		Grid	Min. Temperature
Case-2-	β=9	83932	83.828
		108111	84.31
		123854	84.749
		134317	84.771
	β=25	121234	83.53
		137906	84.025
		149523	84.597
		161873	84.612

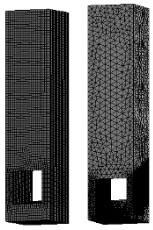

$-a-$ $-b-$

Figure 8. Grid configuration for the case -1- a) $\beta = 8$ b) $\beta = 22$

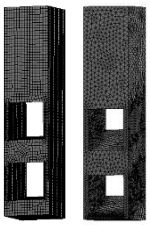

$-a-$ $-b-$

Figure 9. Grid configuration for the case -2- a) $\beta = 9$ b) $\beta = 25$.

7. Results and Discussion

7.1 Validation of analytical model

In the first method, Kirpikov [14] derived the temperature distribution along the perforated fin is a function of the Biot number. Equation to calculate the Biot number of the present model describe as:

$$Bi = \frac{LT^2[\sum hi\, A_{convi}]}{k\int A_{cond}\, dy} \quad i = 1,2,3 \qquad (10)$$

The high similarity between the results are shown below the perforation region, but a spacing was increased between the results in the perforation region. Maximum difference can be reached to (0.52%-0.6%) as shown in Figures (10 and 11) for elliptical and rectangular perforation, respectively.

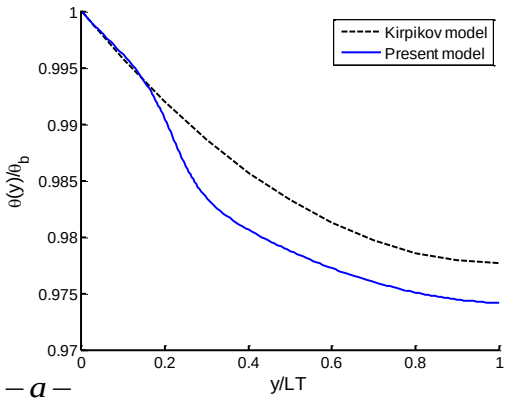

$-a-$

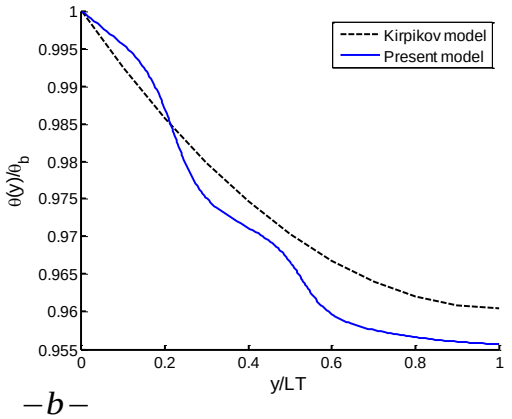

$-b-$

Figure 10. Comparisons between present model and Kirpikov model at $\beta = 0^{\circ}$. a) Case-1- b) Case-2- .

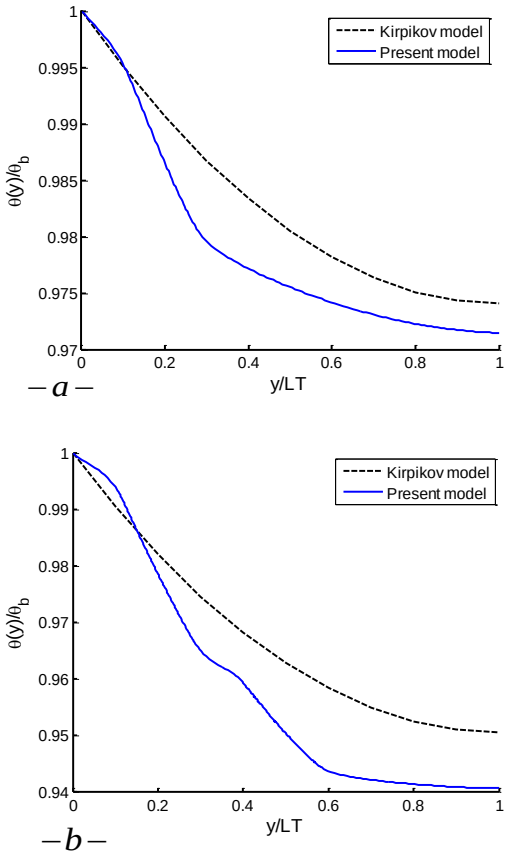

Figure 11. Comparisons between Present model and Kirpikov model at $\beta = 0^{\circ}$. a) Case-1- b) Case-2-.

Furthermore, above the perforation region the results spacing was decreased.

The reasons of the spacing of results can be explained as follows:

1-In Kipikov model, heat transfer coefficient was not classified into three regions.

2- In Kipikov model, approximate solution (Fourier series) was adopted.

3- In Kipikov model, convection coefficient of inner surface was assumed as a ratio from the external coefficient (not depended on the size and length of the perforation).

In the second way of the validation, two inclination angles are adopted for each case that is considered in the calculation process. The distribution of the fin temperature (θ/θ_b) was calculated along the fin length (y/LT) to show the convergence between the analytical solution (by using the present mathematical techniques) and numerical solution (by using Ansys simulation) as shown in Figures (12 and 13) for the elliptical perforation and figures (14 and 15) for rectangular perforation.

Increase each of the inclination angle, size and number of perforations which leads to decrease the temperature of the fin as a result of many reasons:

- Increase of the inner convection area.
- Distribute the inner convection area on the longer length in the y-axis.
- Increase of the external perforated area.
- The conduction area that is replaced by the convection area was increased.

The results show, the temperature profile does not have the classic shape as a result to add convection effects through the conduction cross section area. But, in any case the profile of the results is the same for the analytical and numerical models. In addition, agreements of results are complete resemblance below the fin length 0.2 or 0.3 based on the inclination angle. While, above these limits the a maximum difference can be reached to the (0.33%) .

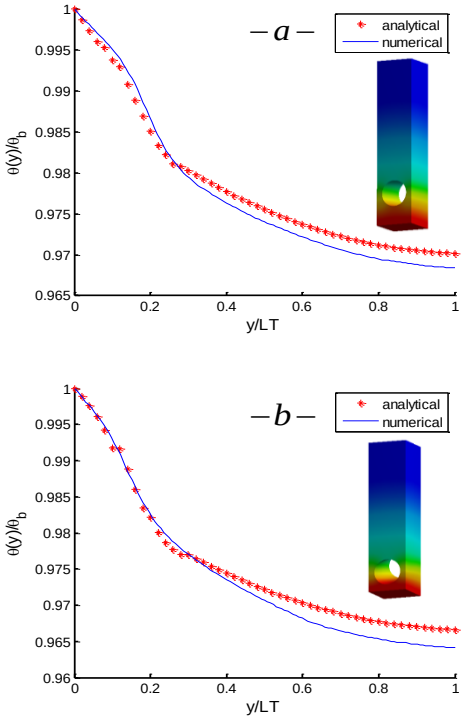

Figure 12. Comparisons between analytical and numerical results for the case-1- a) $\beta = 8^{\circ}$ b) $\beta = 22^{\circ}$.

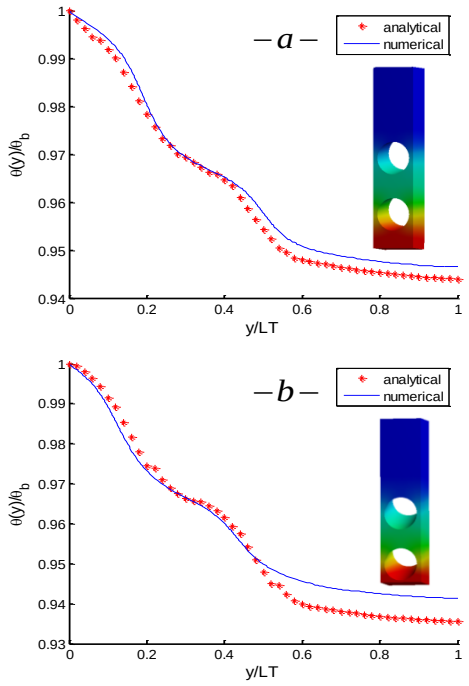

Figure 13. Comparisons between analytical and numerical results for the case-2- a) $\beta = 9^{\circ}$ b) $\beta = 25^{\circ}$.

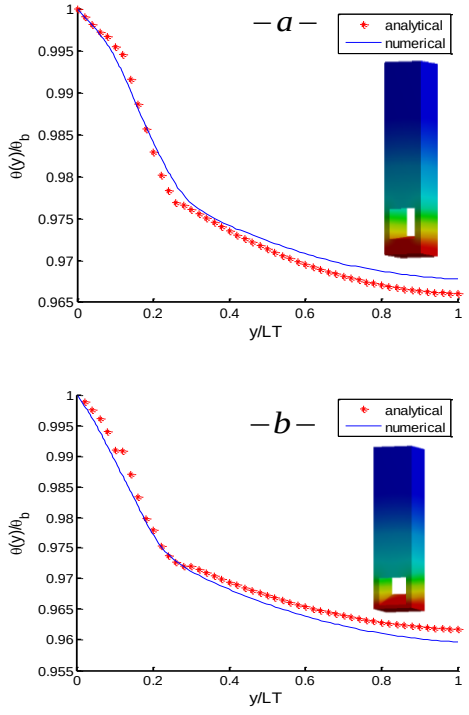

Figure 14. Comparisons between analytical and numerical results for the case-1- a) $\beta = 8^{\circ}$ b) $\beta = 22^{\circ}$.

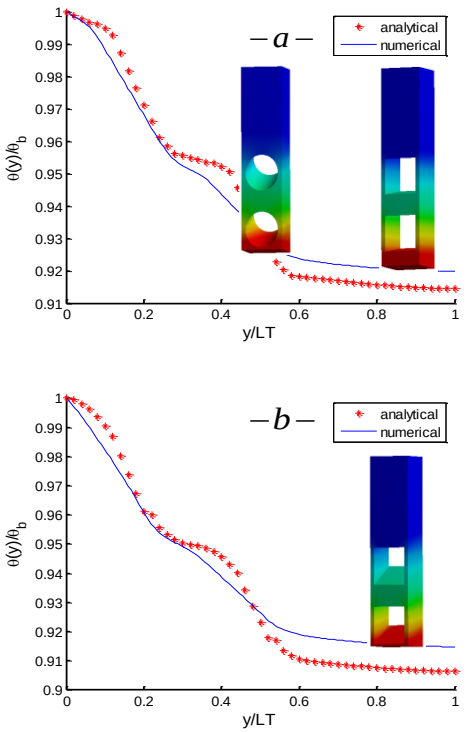

Figure 15. Comparisons between analytical and numerical results for the case-2- a) $\beta = 9^{\circ}$ b) $\beta = 25^{\circ}$.

7.2 Effects of inclination (thermal resistance)

The heat transfer area was changed due to the inclined perforation. Which leads to variable thermal resistance (R_{th}) along the fin length. According to the insulted fin tip, equation to calculate the thermal resistance described as:

$$R_{th} = \frac{A_{conv}}{\int \sqrt{h\,p\,k\,A}\,dA_{conv}\ \tanh\left(\frac{\int \sqrt{h\,p/kA}\,dA_{conv}}{A_{conv}} LT\right)} \tag{11}$$

Where:

$$A_{conv.} = \int_0^{LT} (P_{conv1} + P_{conv2} + P_{conv3})\,dy$$

In inclined perforation region, the conduction area was replaced by the convection area, which leads to improve the thermal resistance. Figures (16 &17) show the result of the thermal resistance with inclination angles for one and two perforations of the elliptical perforation, respectively. While the figures (18

and 19) show the results for one and two perforations of the rectangular perforation, respectively. All results show the decreases of the thermal resistance about (3.9% - 5.2%) with an increase for both the inclination angle and perforation size. Also, using the double perforations leads to improve the thermal resistance about (6.3%) .

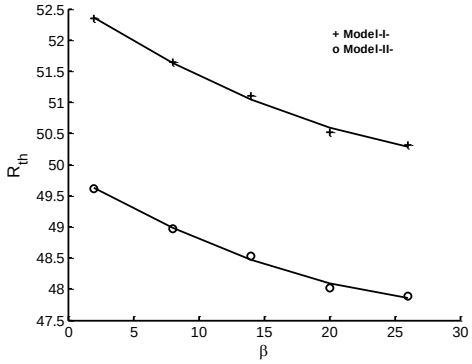

Figure 16. Variation of the R_{th} with inclination angle.

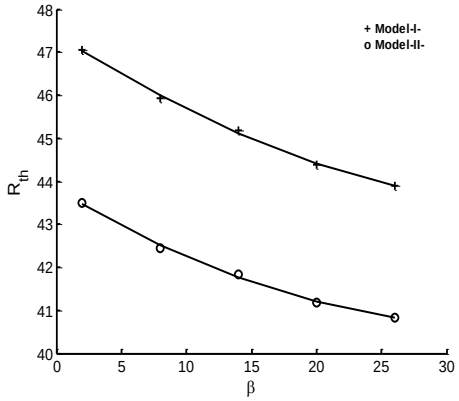

Figure 17. Variation of the R_{th} with inclination angle.

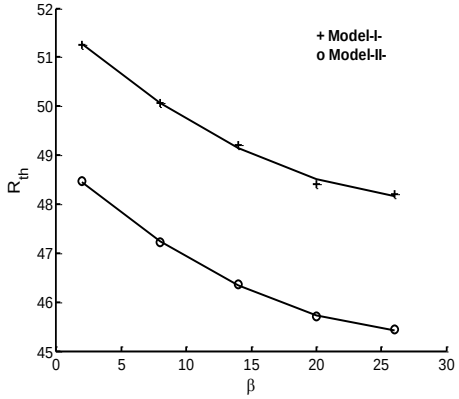

Figure 18. Variation of the R_{th} with inclination angle.

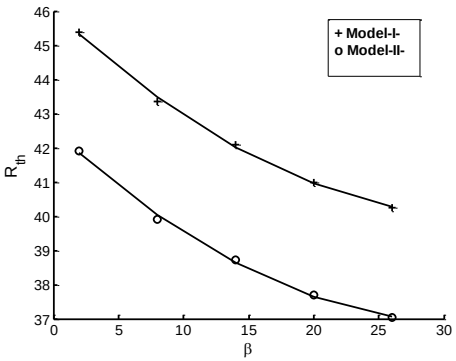

Figure 19. Variation of the R_{th} with inclination angle.

The change of the perforation shape has a less improve about (2%) when compared with the other parameters. But the use of the rectangular perforations leads to better results when compared with an elliptical shape.

7.3 Effects of the inclination (Heat ratio)

The heat transfer ratio q_p / q_s is described as the ratio between the heat transfer of a perforated fin to heat transfer of the solid fin at the same properties and operating conditions.

$$q_{p \ or \ s} = -k \ A_b \left. \frac{d\theta}{dy} \right|_{y=0} \qquad (12)$$

Heat transfer is possible to increase, according to the minimization of the thermal resistance and decreases of the temperature distributions that is obtained from inclined perforation.

Figures (20 and 21) show the increase of the heat transfer ratio about (1.14-1.48) times of the single and double elliptical perforations, respectively. Similarly, Figures (22 and 23) show the increase of the heat transfer ratio about (1.168-1.65) times of the single and double rectangular perforations, respectively.

Increase the inclination angles, size and number of the perforations leads to improve the heat transfer ratio due to the decrease each of the fin temperature and thermal resistance. Also, the change of the shapes of perforation (rectangular and elliptical) leads to more improvement of the thermal performance.

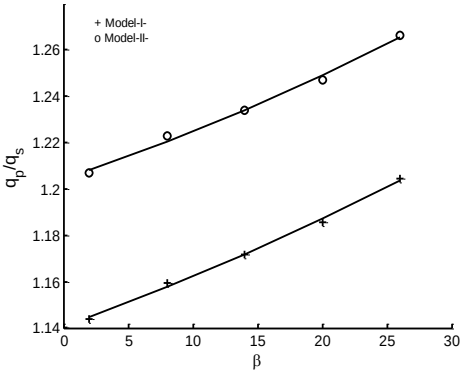

Figure 20. Effects of inclination angles on the heat transfer ratio.

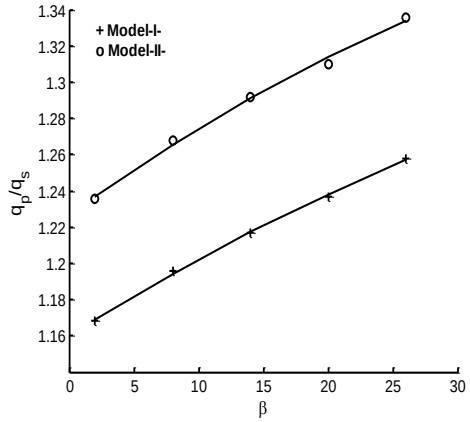

Figure 21. Effects of inclination angles on the heat transfer ratio.

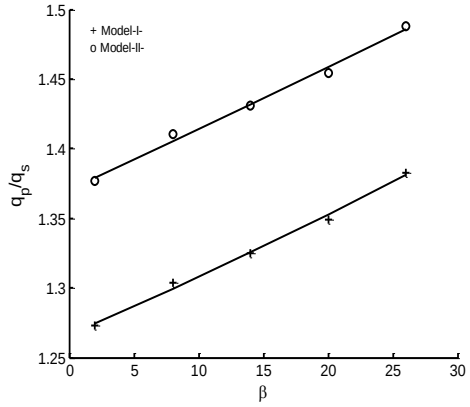

Figure 22. Effects of inclination angles on the heat transfer ratio.

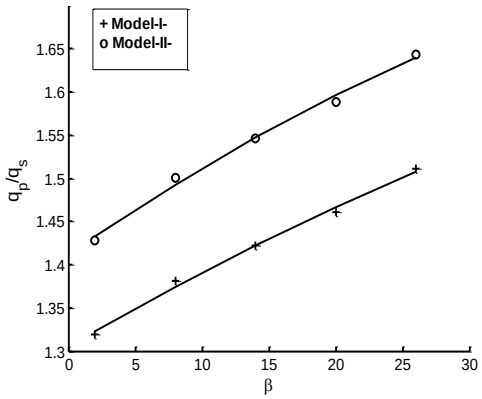

Figure 23. Effects of inclination angles on the heat transfer ratio.

7.4 Effects of the inclination (Effectiveness)

Effectiveness of the inclined perforated fin was increased, according to the decreases of the thermal resistance and increase the heat transfer of the perforated fin when compared with unperforated fin. Figures (24 and 25) show the increase of the effectiveness about (5% - 10%) of the single and double elliptical perforations, respectively. Increased one or all of the parameters (inclination angles and size of perforations) which leads to increase the effectiveness. Also, additional improvement can be achieved when used the double perforations. Likewise, Figures (26 and 27) show the increase of the effectiveness about (8.6% -14%) of the single and double rectangular perforations, respectively. The maximum effectiveness can be reached to the 32.5 of the rectangular perforations and 29.4 of elliptical perforations.

$$\varepsilon = \frac{q_{p\ or\ s}}{q_{no\ fin}} \qquad (13)$$

9. Conclusion

- Many advantages can be achieved with inclined peroration as describe:
  1. Increase of the inner convection area.
  2. Distribute the inner convection area on the longer length in the y-axis.
  3. Increase of the external perforated area.

4. The conduction area that is replaced by the convection area was increased.

- The energy differential equation can be solved by using the DHE and Kummer's series.

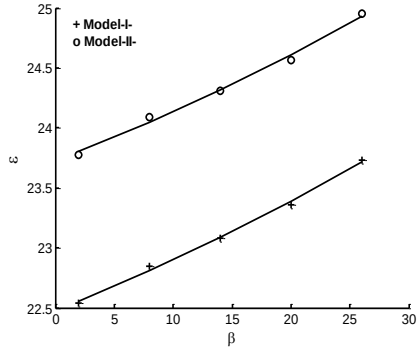

Figure 24. Change the effectiveness with the inclination angles.

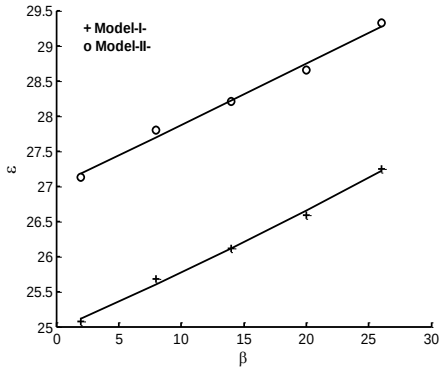

Figure 25. Change the effectiveness with the inclination angles.

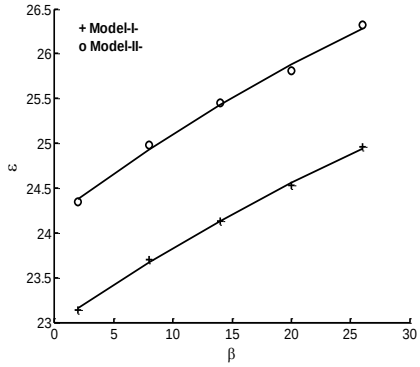

Figure 26. Change the effectiveness with the inclination angles.

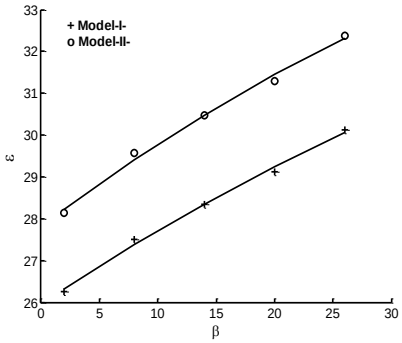

Figure 27. Change the effectiveness with the inclination angles.

- The opposite approach of the variable heat transfer area can be modelled with an especial form of the Signum function.
- The general solution can be taken as the basis to resolve any perforation shape at different specification according to the good agreement of the validation methods and various cases.
- The comparison results show the temperature can be decreased with inclination angle and a maximum drop achieved with inclination angle (25^{o}) of the double perforation.
- Various results suggest that the use of the inclined perforation fin leads to decreased thermal resistance and improve in the thermal performance of the pin fin by enhancing the heat transfer about (65%).
- The change of the perforation shape has a smaller effect on the performance when compared to other parameters that are adopted in this study..

References

1. Saad A. El-Sayed , Mohamed, Abdel-latif, E. Abouda, (2002). Investigation of turbulent heat transfer and fluid flow in longitudinal rectangular-fin arrays of different geometries and shrouded fin array, Experimental Thermal and Fluid Science **26** , 879–900.

2. Rupak k. Banerjee , madhura karve,(2012), evaluation of enhanced heat transfer within a four row finned tube array of an air cooled steam condenser, numerical heat transfer, **61:** 735–753.

3. H. J. Tony tan, m.z. Abdullah and m. Abdul mujeebu (2013), effects of geometry and number of hollow on the performance of rectangular fins

in microchannel heat sinks, J. of Thermal Science and Technology - TIBTD Printed in Turkey.

4. Monoj Baruah, Anupam Dewan and P. Mahanta (2011). Performance of Elliptical Pin Fin Heat Exchanger with Three Elliptical Perforations , CFD Letters Vol. **3(2)** [S2180-1363 (11) 3265.
5. M.R. Shaeri, M. Yaghoubi (2009[a]),Thermal enhancement from heat sinks by using perforated fins , Energy Conversion and Management 50 .
6. M.R. Shaeri, M. Yaghoubi , K. Jafarpur(2009[b]),Heat transfer analysis of lateral perforated fin heat sinks , Applied Energy 86 (2009).
7. Bayram Sahin, Alparslan Demir (2008[a]) . Performance analysis of a heat exchanger having perforated square fins, Applied Thermal Engineering [28 (2008) 621–632]
8. Bayram Sahin, Alparslan Demir (2008[b]) . Thermal performance analysis and optimum design parameters of heat exchanger having perforated pin fins , Energy Conversion and Management [49(2008) 1684-1695].
9. Amol B. Dhumne, Hemant S. Farkade (2013), Heat Transfer Analysis of Cylindrical Perforated Fins in Staggered Arrangement, International Journal of Innovative Technology and Exploring Engineering (IJITEE) , Volume-**2**, Issue-5, April .
10. Saurabh D. Bahadure , Mr. G. D. Gosavi (2014). Enhancement of Natural Convection Heat Transfer from Perforated Fin, International Journal of Engineering research, Volume No.**3**, Issue No.9, pp : 531-535.
11. E. A. M. Elshafei (2010). Natural Convection Heat Transfer from a Heat Sink with Hollow / Perforated-Circular Pin Fins, Energy [35 (2010) 2870e2877].
12. Kavita H. Dhanawade , Vivek K. Sunnapwar and Hanamant S. Dhanawade (2014), Thermal Analysis of Square and Circular Perforated Fin Arrays by Forced Convection, International Journal of Current Engineering and Technology .
13. Ashok Fule, A .M Salwe , A Zahir Sheikh, Nikhil Wasnik (2014), Convective heat transfer comparison between solid and perforated pin fin, international journal of mechanisms and robotics research, Vol. **3**, No. 2, April.
14. Kirpikov.V.A and I.I. Leifman (1972). calculation of the temperature profile of a perforated fin, instituted of chemical apparatus design, Moscow. Vol.**23**, No.2, pp.316-321, August .
15. Abdullah H. M. AlEssa (2009). One-dimensional finite element heat transfer solution of a fin with triangular perforations of bases parallel and towered its base, Arch Appl Mech [79: 741–751].
16. Abdullah H. Al-Essa, Fayez M.S. Al-Hussien (2004) ,The effect of orientation of square perforations on the heat transfer enhancement from a fin subjected to natural convection, Heat and Mass Transfer 40 / 509–515.
17. Kumbhar D.G,Dr.N.K sane , Chavan S.T. (2009), Finite Element Analysis and Experimental Study of Convective Heat Transfer Augmentation from Horizontal Rectangular Fin by Triangular Perforations, international conference on advances in mechanical engineering , National Institute of Technology, Surat - 395 007, Gujarat, India , International Conference on Advances in Mechanical Engineering, [August:376-380] .
18. Mohamed L. Elsayed and Osama Mesalhy (2014), Studying the performance of solid/perforated pin-fin heat sinks using entropy generation minimization,springer-Heat Mass Transfer ,01-12.
19. Incropera, Dewitt, Bergman and Lavine (2007), Fundamental of heat and mass transfer, John Wiley & Sons; 6th edition , [p:95-160 and 560-594].
20. Zan WU, Wei LI, Zhi-jian SUN , Rong-hua HONG (2012), Modeling natural convection heat transfer from perforated plates, Journal of-Zhejiang University-SCIENCE A [13(5):353-360].
21. Raithby GD; Hollands KGT (1998), Natural convection. In: Warren M. Rohsenow, James R Hartnett, Young I. Cho, Handbook of heat transfer, MCGRAW-HILL 3rd edition, [p:4-1 to 4-80].
22. Hisham H. JASIM and Mehmet Sait SÖYLEMEZ (2016[a]), The Temperature Profile for the Innovative Design of the Perforated Fin, Int. Journal of Renewable Energy Development **5(3)** 2016: 259-266.
23. Hisham H. JASIM and Mehmet Sait Söylemez(2016[b]), Enhancement Of Natural Convection Heat Transfer Of Pin Fin Having Perforated With Inclination Angle, J. of Thermal Science and Technology, Isı Bilimi ve Tekniği Dergisi, **36**, 2, 111-118.
24. Andrei D. Polyanin and Valentin F. Zaitsev (2003) , hand book of Exact solution for ordinary differential equations , 2nd ed (USA). By CHAPMAN & HALL/CRC , P.213-490.
25. Hazewinkel. M, (1995), Encyclopaedia of Mathematics: A-Integral- Coordinates, Springer science and business media, [p:105-110 and 797-800].
26. John W. Harris and Horst Stocker (1998), Hand book of mathematics and computational science , springer (USA) [p:130-150].